exothermic reaction become too vigorous. After cooling, the mixture was poured onto ice (200 g) and then allowed to stand overnight. The precipitated solid was filtered off, washed well with cold water, and dried to give 0.38 g (80%) of the 5-nitro derivative **31**: mp (EtOH) 263–266 °C dec; IR ν_{max} (mull) 3500, 3430, 1690 cm^{-1}; ^1H NMR (Me_2SO-d_6) δ 2.24 (3 H, s, Me), 2.55 (3 H, s, Me), 8.18 (1 H, s, aromatic), one midfield, broad exchangeable proton. Anal. ($C_{12}H_8N_4O_4$) C, H, N.

Methylation of 4,9-Dihydro-6,7-dimethyl-4,9-dioxo-1*H*-naphtho[2,3-*d*]-*v*-triazole (16). Anhydrous K_2CO_3 (1.60 g, 11.6 mmol) was added to a solution of **16** (1.135 g, 5 mmol) and MeI (0.5 mL) in dry Me_2NCHO (25 mL), and the mixture was stirred for 1 h at 20 °C. Dilution with water afforded a buff-colored precipitate, which was separated, washed with water, and dried in vacuo over P_2O_5 to give 1.02 g (84%) of N^1-methyl (**32**) and N^2-methyl (**33**) isomers in the ratio 2:1 (from NMR). Chromatography on SiO_2 eluting with $CHCl_3$ gave first the white N-2 isomer **33**: mp ($CHCl_3$–petroleum ether, bp 40–60 °C) 224 °C; IR ν_{max} (mull) 1690, 1685 (shoulder), 1600 cm^{-1}; ^1H NMR ($CDCl_3$) δ 2.40 (6 H, s, C-CH_3), 4.42 (3 H, s, N-CH_3), 8.03 (2 H, s, aromatics). Anal. ($C_{13}H_{11}N_3O_2$) C, H, N.

Further elution gave the pale yellow N-1 isomer **32**: mp ($CHCl_3$–petroleum ether, bp 40–60 °C) 238 °C; IR ν_{max} (mull) 1695 (shoulder) 1685, 1600 cm^{-1}; ^1H NMR ($CDCl_3$) δ 2.42 (6 H, s, C-CH_3), 4.45 (3 H, s, N-CH_3), 7.90 (1 H, s, aromatic), 8.02 (1 H, s, aromatic). Anal. ($C_{13}H_{11}N_3O_2$) C, H, N.

Rat Passive Cutaneous Anaphylaxis. This was carried out by the procedure previously described,[15] except that Charles Rivers' Sprague–Dawley male rats were used. Each dose of a compound was given intravenously to six animals at the time of antigen challenge, the doses being adjusted so that for most compounds three different doses produced an inhibition of between 30 and 70%. The variation in a control group of six animals gave an SEM of about 6%, and inhibitions greater than 20% were usually significant. Regression lines were fitted to each data set plotted against the $\log_{10}$ dose, and the median effective dose associated confidence limits were then estimated as the doses corresponding to a 50% response, as calculated from the equations of the regression line and the 95% confidence limits of the mean response to any given dose.[16]

Acknowledgment. The authors express their appreciation to A. E. Davey and N. J. Morgan for their assistance with some of the syntheses and to D. M. Rose for the statistical analyses.

Registry No. 4, 605-93-6; **5**, 2202-79-1; **6**, 72364-92-2; **7**, 41791-77-9; **8**, 72367-94-3; **9**, 6944-78-1; **10**, 72367-95-4; **11**, 72364-90-0; **12**, 72367-96-5; **13**, 18691-24-2; **14**, 3915-98-8; **15**, 72364-93-3; **16**, 72364-91-1; **17**, 130-15-4; **18**, 79707-02-1; **19**, 79707-03-2; **20**, 72364-96-6; **21**, 72365-05-0; **22**, 80841-91-4; **23**, 84731-20-4; **24**, 84731-21-5; **25**, 84731-22-6; **26**, 80841-85-6; **27**, 72364-95-5; **28**, 84731-23-7; **29**, 84731-24-8; **30**, 84731-25-9; **31**, 72364-98-8; **32**, 84731-26-0; **33**, 84731-27-1; 4-MeOPhCH_2N_3, 70978-37-9; **12** (R_1, R_2 = H), 13755-96-9.

(15) Spicer, B. A.; Ross, J. W.; Smith, H. *Clin. Exp. Immunol.* **1975**, *21*, 419.

(16) Snedecor, G. W.; Cochran, W. G. "Statistical Methods", 7th ed.; Iowa State University Press: Ames, IA, 1980; p 169. Finney, D. J. "Probit Analysis", 3rd ed.; Cambridge University Press: Cambridge, 1971; Chapter 3.

Structure–Activity Correlations for a Series of Antiallergy Agents. 2. Geometric and Electronic Characterization of Some Oxamic and Dioxamic Acids[1]

B. Vernon Cheney,*[,†] David J. Duchamp,[†] and Ralph E. Christoffersen[‡,2]

Research Laboratories of The Upjohn Company, Kalamazoo, Michigan 49001, and Department of Chemistry, University of Kansas, Lawrence, Kansas 66045. *Received June 22, 1982*

Hartree-Fock self-consistent field calculations using the ab initio molecular fragment technique have been performed on some phenyloxamic and *m*-phenylenedioxamic acids, which exhibit markedly different activities in the rat passive cutaneous anaphylaxis (PCA) assay. Attention is focused upon structural features that are most likely to affect the drug–receptor interactions, such as the preferred molecular geometry, the electronic charge distribution, and the nature of the higher occupied (HOMO) and lower unoccupied (LUMO) molecular orbitals. Judging from the regions of high density in HOMOs and LUMOs, the benzene ring would preferably act as an electron acceptor, while the oxamic acid moiety would serve best as an electron donor. Factors affecting the relative PCA activities of oxamic and dioxamic acids are discussed.

A number of oxamic and dioxamic acids, resembling structures **1** and **2**, have been shown to inhibit the allergic response that follows antigen–antibody reaction on sensitized mast cells.[1,3] Although the site of action has not been identified unequivocally, an agent with a similar spectrum of biological effects (cromolyn sodium) has been observed to associate reversibly with the mast cell.[4,5] Since no penetration of cromolyn sodium into the interior cell was detected, it appears that the entity with which the drugs interact may be located on, or within, the cellular membrane. In any case, the drugs ultimately block release of the mediators of the allergic reaction from the triggered mast cell. Activity of this type may be measured in a

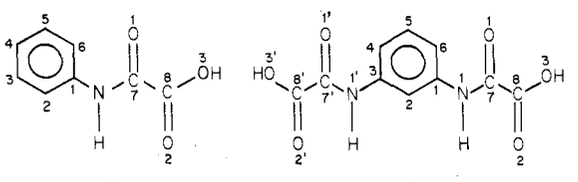

1 **2**

† The Upjohn Co.
‡ University of Kansas.

(1) For the previous paper in this series, see B. V. Cheney, J. B. Wright, C. M. Hall, H. G. Johnson, and R. E. Christoffersen, *J. Med. Chem.*, **21**, 936 (1978).
(2) Present address: Colorado State University, Fort Collins, CO 80523.
(3) J. B. Wright, C. M. Hall, and H. G. Johnson, *J. Med. Chem.*, **21**, 930 (1978).
(4) H. G. Johnson and C. A. VanHout, *Proc. Soc. Exp. Biol. Med.*, **143**, 427 (1973).
(5) C. M. Hall and H. G. Johnson in "Drugs Affecting the Respiratory System" (*ACS Symp. Ser.*, **no. 118**), D. L. Temple, Jr., Ed., American Chemical Society, Washington, D.C., p 69.

0022-2623/83/1826-0719$01.50/0

straightforward manner by the rat passive cutaneous anaphylaxis (PCA) assay.[6]

A quantitative index for the biological effect of a compound is provided by the ED_{50}, which represents the dose required to produce 50% inhibition of the anaphylactic reaction in the PCA test. The respective ED_{50} values for oxanilic acid (1) and *N,N'*-(*m*-phenylene)dioxamic acid (2) are 245 and 0.40 μmol/kg of rat body weight. Thus, 2 is 600-fold more potent than 1. An even greater increase in activity is achieved with *N,N'*-(2-chloro-5-cyano-*m*-phenylene)dioxamic acid (3), which exhibits an ED_{50} of 2.3 nmol/kg of rat body weight.

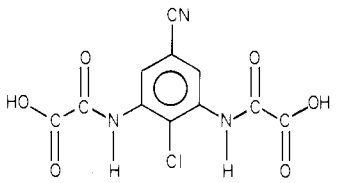

3

In the previous report,[1] a quantitative structure–activity relationship was established between biological activity in the PCA assay and the energy of a low-lying unoccupied orbital in a series of compounds exhibiting features similar to 1. For that series, a single parameter sufficed to fit the experimental data. In order to rationalize the correlation, it was proposed that charge-transfer stabilization of the drug–receptor complex plays a major role in determining the potency of agents related to the oxamic acids. The evidence supplied by the correlation indicates that the antibonding π orbital (which is localized within the phenyl moiety) serves as an electron acceptor in the complex. However, a relatively weak, ring-centered charge-transfer interaction cannot provide a complete explanation for the tremendous variation in potency between the oxamic and dioxamic acids. Hence, an understanding of other factors affecting biological activity must be obtained through detailed analysis of structural differences among these molecules. As a means of characterizing the structures, ab initio SCF–MO calculations have been performed on molecules 1–3, as well as a few other congeners, utilizing the molecular fragment technique.[7] The subject of this paper concerns the results of the calculations, which reveal several interesting electronic and geometric features of possible importance to drug action.

Results

SCF–MO Computations. The basis functions employed in the ab initio molecular fragment method consist of floating spherical Gaussian orbitals (FSGO), which have been described elsewhere.[8,9] Molecular orbitals (MOs) for the system are written as linear combinations of the basis functions by using eq 1, where N is the number of FSGO

$$\phi_i = \sum_s^N c_{si} G_s \tag{1}$$

basis functions, G_s, and c_{si} is an expansion coefficient to be determined. Optimization of the molecular wave function is performed by a standard self-consistent field (SCF) procedure.[10] The elements of the charge-density and bond-order matrix were calculated by eq 2, where the

$$P_{st} = \sum_i^{occ} c_{si} c_{ti} \tag{2}$$

summation includes all occupied molecular orbitals. Convergence of the iterative process was considered to be achieved when successive values of P_{st} differed in magnitude by less than 10^{-4}.

Analysis of the electronic structure may be carried out by expressing the molecular wave function in terms of symmetrically orthogonalized basis functions, χ_r, defined by eq 3, where $S_{sr}^{-1/2}$ is an element of the unitary transformation matrix that diagonalizes the FSGO overlap matrix.[11,12] In the symmetrically orthogonalized representation, electron populations and bond orders are given, respectively, by the diagonal and off-diagonal terms of $\mathbf{P}'$, a matrix computed by the following transformation:

$$\chi_r = \sum_s^N S_{sr}^{-1/2} G_s \tag{3}$$

$$\mathbf{P}' = \mathbf{S}^{1/2}\mathbf{P}\mathbf{S}^{1/2} \tag{4}$$

Correlations between MOs from different molecules may be expressed in terms of the index τ_{ij}^2, given by the relationship shown in eq 5. In eq 5, C_{ri}^A represents the coefficient of χ_r in the ith MO of molecule A. The terms in eq 5 only arise from corresponding symmetrically orthogonalized basis functions in molecules A and B; if χ_r in molecule A has no counterpart in molecule B, the value of C_{ri}^B is taken to be zero. The magnitude of τ_{ij}^2 will range from 0 to 1 depending upon the degree of similarity between ϕ_i^A and ϕ_j^B.

$$\tau_{ij}^2 = |\sum_r C_{ri}^A C_{rj}^B|^2 \tag{5}$$

It is of interest to examine those features of the electronic structure that are most likely to play a role in determining how molecules 1–3 interact with the receptor. For example, the electronic distribution reveals centers with excess (deficient) populations where electrophilic (nucleophilic) attack may preferentially occur. In addition, the high-energy MOs of the molecules may be investigated to discover whether the molecules are suited to engage in donor–acceptor interactions at the receptor. The energy, ϵ_i, of the ith MO provides an indication of the orbital's capacity to serve as an electron donor if ϕ_i is a higher occupied molecular orbital (HOMO), or an acceptor if ϕ_i is a lower unoccupied molecular orbital (LUMO). Furthermore, sites of high density in ϕ_i reveal where overlap with the complementary receptor MO must occur to permit any significant donor–acceptor interaction.

Molecular Geometry. The bond lengths and angles for all of the molecules under study have been adapted from the crystal structure of diethyl *N,N'*-(*m*-phenylene)dioxamate, which was determined by one of the authors (D.J.D.) using X-ray techniques. A tabulation of the structural data used in the calculations has been reported previously.[1]

Although the possibility of extended conjugation might be expected to stabilize molecules 1–3 in a planar form, the solid-state structure of the diethyl ester of 2 displays two features indicative of some conformational flexibility. First, while the oxamate chains (excluding the terminal ethyl groups) are found to be planar in the crystal, there is an angle of 32.31° between the normal to the plane of

(6) J. Goose and A. M. J. N. Blair, *Immunology*, 16, 749 (1969).
(7) R. E. Christoffersen, D. Spangler, G. G. Hall, and G. M. Maggiora, *J. Am. Chem. Soc.*, **95**, 8526 (1973).
(8) L. L. Shipman, R. E. Christoffersen, and B. V. Cheney, *J. Med. Chem.*, 17, 583 (1974).
(9) B. V. Cheney and T. Tolly, *Int. J. Quantum Chem.*, 16, 87 (1979).
(10) (a) C. C. J. Roothaan, *Rev. Mod. Phys.*, **23**, 69 (1951). (b) G. G. Hall, *Proc. R. Soc. London, Ser. A.*, **205**, 541 (1951).
(11) P.-O. Löwdin, *J. Chem. Phys.*, 18, 365 (1950).
(12) L. L. Shipman and R. E. Christoffersen, *Chem. Phys. Lett.*, **15**, 469 (1974).

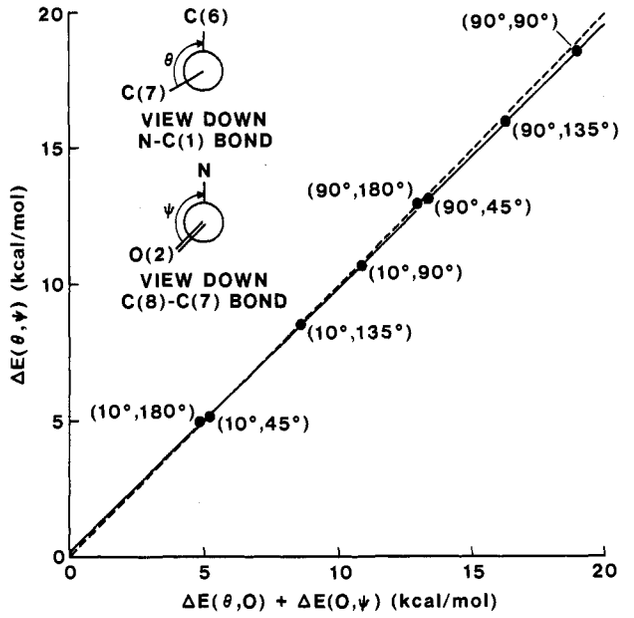

Figure 1. Comparison of conformational energies calculated following simultaneous variation of θ and ψ with the sum of the energies found when the angles are varied independently.

each chain and that of the ring. The orientation of the oxamate groups (which are extended as shown in **2**) confers C_2 symmetry upon the molecule. Second, the C(7)–C(8) and C(7′)–C(8′) internuclear distances are each 1.5326 Å, which falls within the range commonly observed for single bonds. The apparent low degree of double-bond character in the oxalyl C–C linkages could signify the existence of some rotational freedom at those sites. As a result of these considerations, calculations were carried out to investigate factors affecting rotation about the C(1)–N and C(7)–C(8) bonds using oxanilic acid (**1**) as a model system. In order to simplify computations, the concept of rigid rotation was adopted; i.e., bond lengths and angles within each rotating moiety were not permitted to relax for different settings of the torsional angles. Although rigid rotation undoubtedly leads to overestimation of an energy barrier arising from a crowded configuration, this is not of major concern for the torsional angles considered here.

The Newman projections in Figure 1 provide definitions of the torsional angles, θ and ψ, which respectively describe rotation about the C(1)–N and C(7)–C(8) axes. As a means of determining whether θ and ψ could be varied independently or not, several points were calculated on the two-dimensional conformational energy surface. Each of these conformational energies was then compared with the sum of the two energies obtained when one angle was varied by the appropriate amount and the other was fixed at the reference value of 0°. If there is no coupling of the motions, this conformational energy sum would be equal to the quantity found by direct calculation with simultaneous variation of θ and ψ. A graphical representation of such a relationship would yield a line with unit slope and zero intercept. As shown in Figure 1, the actual regression line exhibits a slope of 0.97 and an intercept of 0.2. Since the correlation coefficient is 0.9999 and the standard deviation of points from the line is 0.08, the analysis indicates that the degree of coupling is negligible. Hence, rotations about the C(1)–N and C(7)–C(8) bonds were considered separately in greater detail.

Figure 2 is a portrayal of the rotational barrier obtained by variation of θ in oxanilic acid. A maximum of 8.0 kcal/mol occurs at θ = 90°. There appears to be some allowance for wobble about the C(1)–N bond, since θ may

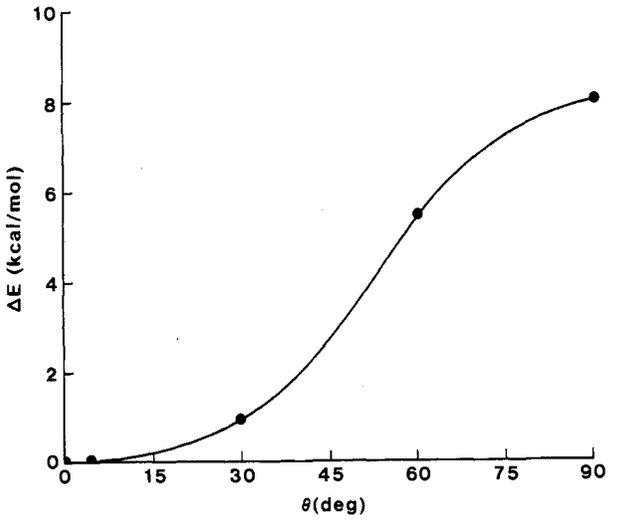

Figure 2. Rotational barrier generated by variations of θ in molecule 1 while ψ remains fixed at 0°.

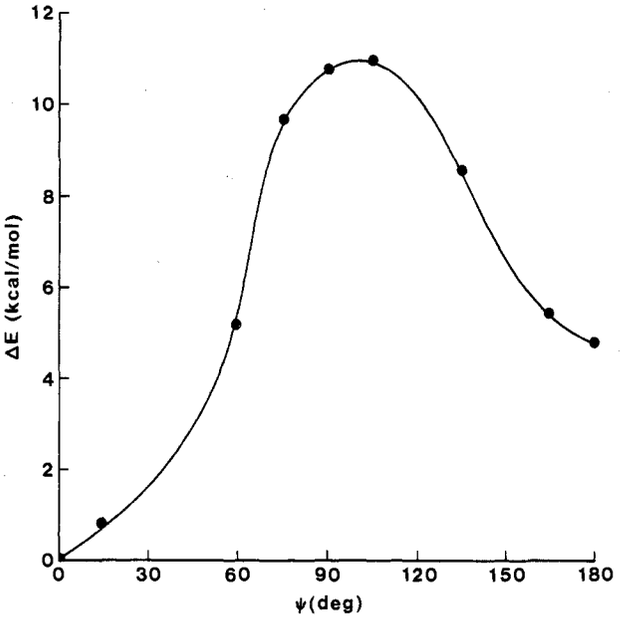

Figure 3. Rotational barrier generated by changing ψ in molecule 1 with θ = 0°.

assume values as large as 10° with essentially no change in conformational energy. The gentle slope of the curve near 0° undoubtedly results from a compromise between competing resonance and steric effects. A planar conformation would be stabilized by the existence of extended conjugation throughout the ring and attached chain. However, rotation from the plane would tend to reduce the steric repulsion between O(1) and H(6). As θ varies from 10 to 90°, the O(1)–H(6) interaction becomes much less important, while continued loss of resonance leads to a steep, high barrier. The nature of this barrier permits some understanding for the large value of θ observed in the solid-state structure of molecule **2**, since moderate crystal-field forces could easily induce a rotation through 32°.

In Figure 3, an illustration is given of the effect of changes in ψ upon the conformational energy of molecule **1**. The rotational potential function exhibits a maximum of 10.9 kcal/mol at 105° with a primary minimum at 0° and a secondary minimum at 180°. The conformer with the carbonyl oxygens, O(1) and O(2), in a trans relationship is favored by 4.8 kcal/mol. Although the C(7)–C(8) linkage

Table I. Calculated Effect of Various Ortho Substituents on Conformational Energies of Planar Oxanilic Acid Stereoisomers

substituent	conformational energy[a] anti	syn
CN	0.0	140.7
F	0.0	27.6
Cl	0.0	169.1

[a] Energy in kilocalories per mole relative to the calculated ground-state conformation. The nomenclature for the two planar forms is described in the text.

corresponds closely to a single bond in length, the sharp rise of the barrier at $\psi = 0°$ implies that rotation about this bond would be quite restricted. Thus, the oxamic acid group should generally assume a near-planar conformation as observed in the crystal structure of the diethyl ester of molecule **2**.

In view of the apparent repulsive interaction between H(6) and O(1), the effect of an ortho substituent other than hydrogen merits some consideration. The planar structures of such a molecule may be defined as anti and syn forms according to the following convention:

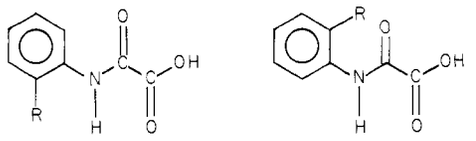

anti syn

As shown in Table I, the R–O(1) steric repulsion is severe for the syn conformation when R = F, Cl, or CN. Hence, such ortho-substituted molecules are predicted to be locked in the anti form.

Molecule **2** may exist in three stereoisomeric planar structures, designated hereafter as the anti–anti (aa),

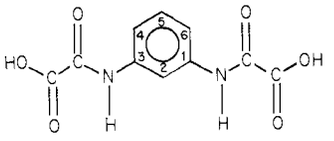

aa

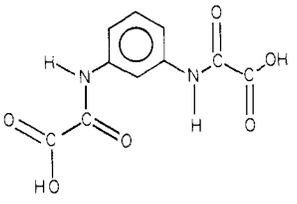

sa

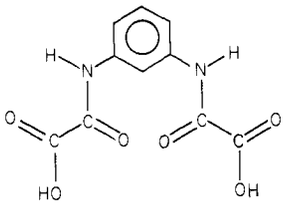

ss

syn–anti (sa), and syn–syn (ss) conformations. Calculations indicate that the sa structure should be more stable than the others in vacuo, although the ss form is only 0.1 kcal/mol higher in energy. The aa conformer, which is most similar to the crystal structure, is predicted to be 1.1 kcal/mol less stable than the sa. Judging from the small differences in energy for the three conformations, the oxamic acid moieties do not appear to interact strongly with one another. As a result, in the biological medium, interactions with the surrounding solvent molecules and the receptor could play a decisive role in determining the favored conformation for binding.

Based on the information given in Table I, the presence of relatively bulky substituents ortho to one, or both, of the ring appendages will impose certain conformational

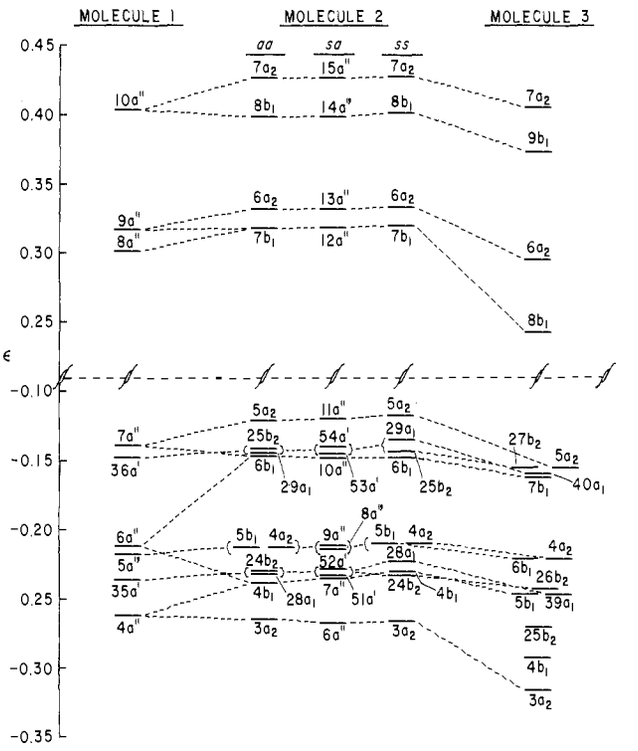

Figure 4. Energies, ϵ, of several high-lying occupied and low-lying unoccupied molecular orbitals of the molecules under study. All MOs with negative energy are filled, while those with positive energy are empty. Correlated orbitals with $\tau_{ij}^2 \geq 0.2$ are connected by dashed lines. There is essentially 1:1 correspondence between the π MOs of a given symmetry (a_2 or b_1) in molecules **2** and **3**. Furthermore, most a″ MOs in the sa form of molecule **2** are strongly correlated ($\tau_{ij}^2 \geq 0.7$) with the associated orbitals of higher symmetry in the aa and ss forms, the only exceptions being the 8a″ and 9a″ MOs.

restrictions on the *m*-dioxamic acid system. For example, insertion of F, Cl, or CN at the 2-position of the ring, ortho to both chains, fixes the system in the aa conformation. This is the case with molecule **3**. If the substituent is located at the 4-position, the molecule may take the sa or the ss form, but cannot assume the aa conformation. Furthermore, only the ss conformation is available to a molecule with bulky substituents in both the 4- and 6-position of the ring.

Electronic Structure. Comparisons of electron populations and bond orders for the σ and π systems of molecules **1**–**3** are shown in Tables II and III, where the findings are reported in terms of the symmetrically orthogonalized representation. (See paragraph at the end of paper concerning supplementary material.) Consideration of the σ system, listed in Table II, reveals that large bond orders (with absolute value ≥0.25) exist only for pairs of symmetrically orthogonalized functions located in the bonding regions between adjacent atoms. In addition, when comparisons are limited to features in the structural moiety common to all three molecules, it is seen that the σ system remains remarkably constant; in no case does a particular index of the σ-electron distribution vary by more than 1% from one molecule to another. Examination of the π-electron occupation numbers and bond orders (see Table III) reveals a significantly greater accumulation of charge on C(2), C(4), and C(6) in molecules **2** and **3** than in molecule **1**. It appears that the N(1) lone-pair orbital feeds electrons into the π system of the aromatic ring, where the excess charge is deposited on the ortho and para carbons. This effect is magnified in the dioxamic acids, since the migration from N(1′) reinforces the transfer from

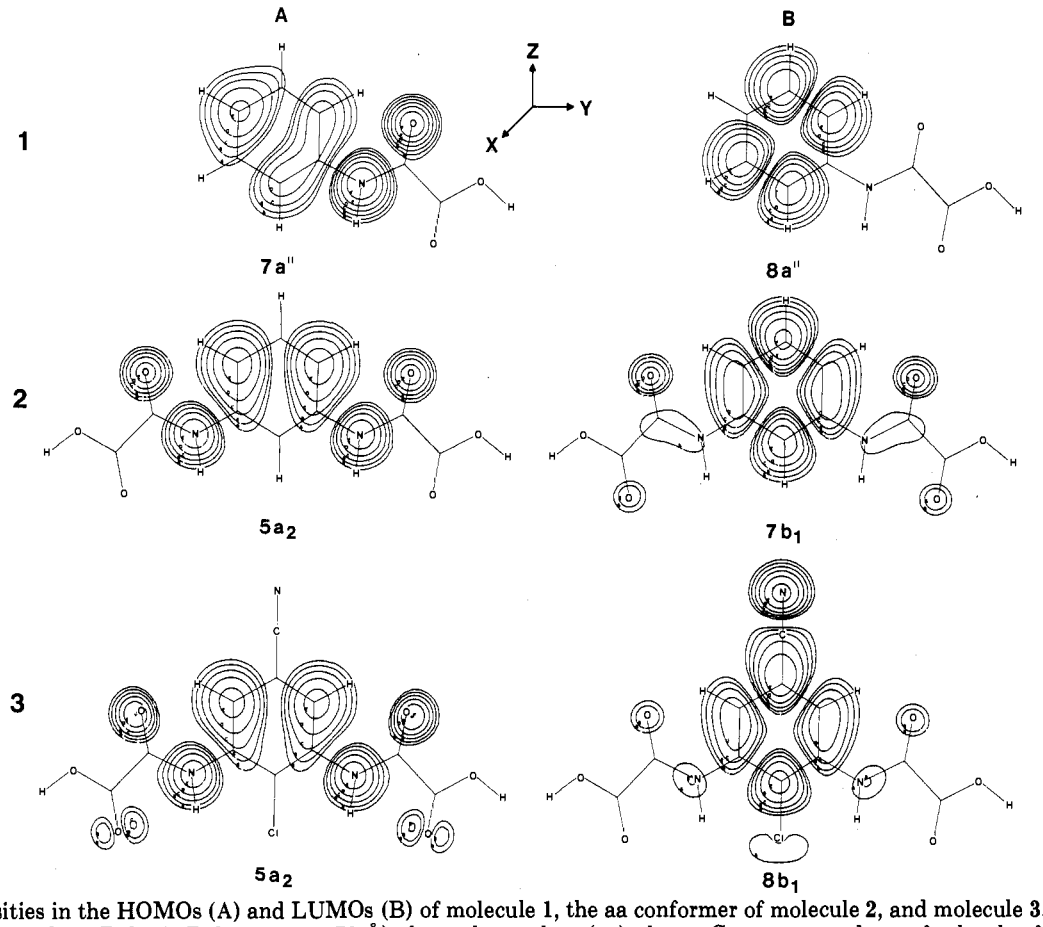

Figure 5. Densities in the HOMOs (A) and LUMOs (B) of molecule **1**, the aa conformer of molecule **2**, and molecule **3**. The section of the map is located 0.8 Bohr (1 Bohr = 0.529172 Å) above the nuclear (yz) plane. Contours are drawn for levels of 1, 2, 4, 8, 16, 32, and 64 millielectrons per cubic Bohr. Molecules **2** and **3** exhibit C_{2v} symmetry, and the z axis is taken to be the 2-fold rotation axis in these drawings.

N(1). In contrast to the situation in the aromatic ring, little variation occurs from molecule to molecule in the π populations and bond orders of corresponding centers in the oxamic acid chain. In each of the three molecules, the π bond orders provide evidence for extensive delocalization over the aromatic ring and the amide moiety. Within the carboxy group, the π electrons are also delocalized over C(8), O(2), and O(3). However, the CO_2H entity is isolated from the remainder of the π system due to the small (0.173) π bond order of the C(7)–C(8) linkage. Of some interest is the fact that the total calculated C(7)–C(8) bond order agrees well with the experimental finding of a single-bond internuclear distance.

In Figure 4, the energies of several HOMOs and LUMOs in molecules **1**–**3** are shown along with correlations between the MOs of greatest similarity as determined by the τ_{ij}^2 index. As shown in Table IV, several π MOs are interspersed among the high-lying, nonbonded (n) molecular orbitals, which are composed primarily of lone-pair, l_p and l_σ, functions on O(1), O(2), and O(3). Some MOs contain substantial contributions from p_π-type lone-pair functions on N(1) and O(3). In molecules **2** and **3**, the basis functions associated with the second oxamic acid chain provide MO contributions equivalent to their counterparts in the first chain, although slight differences occur in the case of the sa form of *N,N'*-(*m*-phenylene)dioxamic acid. Comparison of the oxamic acid, **1**, with the dioxamic acid, **2**, reveals a resonance splitting of the n-type orbitals in the latter molecule. The correlation index reflects this situation, since $\tau_{ij}^2 = 0.5$ for the match of an MO having a′ symmetry in **1** with the corresponding a_1 and b_2 MOs in **2**. Resonance splitting of a π orbital is also indicated by the value of 0.5 obtained for τ_{ij}^2 in the match of the 5a″ MO in **1** with the $4a_2$ and $5b_1$ MOs in **2**. These π MOs are restricted to the carboxy groups in the two molecules. Correlations with $\tau_{ij}^2 \geq 0.6$ result from matches of the HOMO, LUMO, and LUMO+1 in molecule **1** with their counterparts in molecule **2**. These MOs exhibit high density in the π system of the benzene ring and, except for the LUMO, of the amide group(s). Values of τ_{ij}^2 obtained from comparison of molecules **2** and **3** reveal nearly 1:1 correspondence between the symmetry-related MOs of similar energy, which are connected by dashed lines in Figure 4.

Since the HOMO and LUMO are best suited from an energy standpoint to participate in charge-transfer interactions, it is interesting to note that the correlation index highlights the similarity of the drugs under study with respect to these two features. In order to provide a visual comparison of the frontier molecular orbitals, contour density maps of the HOMO and LUMO in each of the three molecules are shown in Figure 5. Since all of the HOMOs are much alike within a large moiety that contains points of high density at N(1), O(1), C(1), C(4), and C(6), the drugs seem to be well suited to act as donors in charge-transfer interactions at a common receptor. The only difference of particular note in the HOMOs has to do with the region surrounding C(2). This carbon atom is a site of significant electron density in the 7a″ MO of **1**; however, due to the antisymmetry of the $5a_2$ MOs with respect to reflection in the XZ plane, C(2) is a nodal point devoid of electronic charge in the HOMOs of **2** and **3**. In considering the LUMOs of molecules **1**–**3**, it is seen that most of the density distribution is concentrated in the aromatic ring at C(2), C(3), C(5), and C(6). Nodal surfaces

Table IV. Descriptions of High-Energy Molecular Orbitals in the Molecules of Interest

molecule 1				molecule 2[a]				molecule 3			
ϕ_i[b]	type[c]	energy[d]	sites of high density[e]	ϕ_i[f]	type[c]	energy[d]	sites of high density[e]	ϕ_i[f]	type[c]	energy[d]	sites of high density[e]
9a''	π^*	0.3170	C(1), C(4), O(1), C(3), C(5), C(7), C(6), C(2)	$6a_2$	π^*	0.3316	C(1), C(3), C(4), C(6), O(1), O(1'), C(7), C(7')	$6a_2$	π^*	0.2953	C(1), C(3), C(4), C(6), O(1), O(1'), C(7), C(7')
8a''	π^*	0.3011	C(5), C(3), C(2), C(6)	$7b_1$	π^*	0.3187	C(5), C(2), C(1), C(3), C(4), C(6)	$8b_1$	π^*	0.2429	C(5), C(2), N(2), C(4), C(6), C(9), C(1), C(3)
7a''	π	−0.1387	N(1), C(4), C(2), O(1), C(6), C(1)	$5a_2$	π	−0.1211	C(4), C(6), N(1), N(1'), C(3), C(1), O(1), O(1')	$5a_2$	π	−0.1561	C(4), C(6), N(1), N(1'), O(1), O(1'), C(1), C(3)
36a'	n	−0.1475	O(1), O(2), C(7), C(8), O(3)	$25b_2$	n	−0.1411	O(1), O(1'), O(2), O(2'), C(8), C(8'), C(7), C(7'), O(3), O(3')	$27b_2$	n	−0.1564	O(2), O(2'), O(1), O(1'), O(3), O(3')
6a''	π	−0.2115	C(6), C(3), C(2), C(4)	$29a_1$	n	−0.1439	O(1), O(1'), O(2), O(2'), C(8), C(8'), C(7), C(7'), O(3), O(3')	$40a_1$	n	−0.1585	O(2), O(2'), O(1), O(1'), O(3), O(3')
5a''	π	−0.2170	O(3), O(2), C(8)	$6b_1$	π	−0.1465	C(2), N(1), N(1'), O(1), O(1'), C(5)	$7b_1$	π	−0.1618	C(2), Cl(1), N(1), N(1'), C(5), O(1), O(1')
35a'	n	−0.2356	O(1), O(2), O(3)	$4a_2$	π	−0.2135	O(2), O(2'), O(3), O(3'), C(8), C(8')	$4a_2$	π	−0.2214	O(2), O(2'), O(3), O(3'), C(8), C(8')
4a''	π	−0.2617	O(1), C(4), N(1), C(1), C(7), C(5), C(3)	$5b_1$	π	−0.2138	O(2), O(2'), O(3), O(3'), C(8), C(8')	$6b_1$	π	−0.2214	O(2), O(2'), O(3), O(3'), C(8), C(8')
				$24b_2$	n	−0.2294	O(1), O(1'), O(2), O(2'), O(3), O(3')	$26b_2$	n	−0.2439	O(1), O(1'), O(2), O(2'), O(3), O(3')
				$28a_1$	n	−0.2324	O(1), O(1'), O(2), O(2'), O(3), O(3')	$39a_1$	n	−0.2463	O(1), O(1'), O(2), O(2'), O(3), O(3')
				$4b_1$	π	−0.2381	C(5), C(4), C(6), N(1), N(1'), C(2), O(1), O(1')	$5b_1$	π	−0.2476	N(1), N(1'), C(5), O(1), O(1'), Cl(1), N(2), C(4), C(6)
				$3a_2$	π	−0.2648	O(1), O(1'), C(1), C(3), N(1), N(1'), C(7), C(7'), C(4), C(6)	$25b_2$	n	−0.2708	Cl(1)
								$4b_1$	π	−0.2938	Cl(1), N(2), C(5), C(4), C(6), C(9), C(2)
								$3a_2$	π	−0.2949	O(1), O(1'), C(1), C(3), C(7), C(7'), C(4), C(6), N(1), N(1')

[a] The aa form of molecule 2 was employed. In general, correlations with orbitals of corresponding symmetry in the ss form give $\tau_{ij}^2 \geq 0.9$. High correlations are also found with the MOs of the sa conformer, although the loss of C_{2v} symmetry leads to an intermixing of nearly degenerate n-type orbitals as shown in Figure 4. [b] Molecule 1 has C_s symmetry. The HOMO is the 7a'' orbital. [c] The label n is employed for molecular orbitals dominated by contributions from lone-pair basis functions of the type $l_o(X)$ and $l_p(X)$, which are defined in footnote *d* of Table II. The symbol π denotes bonding MOs with strong contributions from p_π functions on the benzene ring carbons and the atoms of the oxamic acid chains. Antibonding MOs dominated by p functions are represented by π^*. [d] The MO energy is reported in atomic units. [e] Sites are listed in decreasing order of importance as indicated by the size of the basis orbital coefficients in the symmetrically orthogonalized representation. [f] C_{2v} symmetry characterizes the system. The HOMO is the $5a_2$ orbital.

separate C(2) and C(5) from neighboring centers of high density in these low-lying antibonding MOs. Therefore, the lowest unoccupied MOs of molecules **1–3** apparently resemble one another sufficiently to serve as acceptors in charge-transfer interactions with a common donor. There are, however, some differences in the LUMOs of the molecules that should be pointed out. For example, C(1) and C(4) contribute significantly to the $7b_1$ and $8b_1$ MOs of **2** and **3**, respectively, but not at all to the 8a″ MO of **1**. Furthermore, the cyano substituent, which is lacking in molecules **1** and **2**, makes a substantial contribution to the $8b_1$ MO in the molecule **3**.

Structure-Activity Considerations. In the previous study,[1] which included several congeners of molecule **1**, the energy, ϵ_a*, of an antibonding MO with the characteristics of the 8a″ orbital was found to correlate linearly with a biological activity index, $A = -\ln ED_{50}$, obtained from the rat PCA assay. The relationship, eq 6, between ϵ_a* and

$$A = -64.4\epsilon_a^* + 28.0 \quad (6)$$

A was explained in terms of charge-transfer stabilization of the drug–receptor complex, where the 8a″ MO in the benzene ring acts as an electron acceptor. The essential pharmacophore of the series of compounds examined in ref 1 was defined in terms of fragment I, which possesses

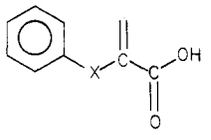

I, X = O or NH

the following features: (a) a planar system with extended π bonding, (b) a benzene ring, (c) an attached oxygen or nitrogen heteroatom, and (d) a carboxy group separated from the heteroatom by the sp^2-hybridized carbon atom marked with an incomplete double bond in the diagram.

Although the dioxamic acids contain moiety I, it may easily be shown that molecules **2** and **3** do not fit the established structure–activity correlation. For example, if the LUMO energy for any of the three conformers of molecule **2** is employed in eq 6, the value of A_{calcd} turns out to be lower than that for molecule **1**, contrary to experimental findings. However, calculation of A for molecule **3** using the energy of the $8b_1$ MO yields a value that is larger than the activity indexes obtained for molecules **1** and **2** in accordance with observation. Nevertheless, the magnitude of A_{calcd} for molecules **2** and **3** is in each case much smaller than A_{obsd}. Thus, the simple structure–activity expression, eq 6, seems to account for the relative activity of molecules **2** and **3** but fails to explain the tremendous enhancement in potency exhibited by the dioxamic acids in comparison to oxanilic acid.

The minor differences in electron distribution among the LUMO orbitals of molecules **1–3** are unlikely to affect overlap with a donor orbital to an extent that would produce any drastic variations in the charge-transfer contribution to the stabilization energy of the drug–receptor complex. Hence, the cause for the enhanced activity of the dioxamic acids must be attributed to attractive interactions between some feature of the receptor and the 3-$NHCOCO_2H$ group. In general, a substituent added to the essential structural moiety, I, may affect the activity in the following two ways: *indirectly* as a result of perturbing critical elements in the electronic structure of the primary pharmacophore and *directly* through encountering a receptor entity with which it strongly interacts by virtue of its own electronic properties. Both the nature of the substituent and the site of attachment on I are important for the attainment of a significant direct effect. In the series of compounds employed to develop eq 6, a variety of substituents were tried in ring positions 2–6 with no noticeable direct effects. However, only CN was used to replace H in the 3-position, and this substituent seemingly fails to interact with a receptor entity that is accessible to the more extended 3-$NHCOCO_2H$ group.

The finding of a significant direct effect by the *m*-oxamic acid group in molecules **2** and **3** suggests that other molecules incorporating the structural elements of these dioxamic acids may be used effectively as probes in a further effort to "map" the receptor. A quantitative structure–activity study involving a number of such drugs is reported in the following paper in this issue.

Acknowledgment. The authors express their appreciation to Drs. W. J. Wechter, J. B. Wright, C. M. Hall, and H. G. Johnson for many helpful discussions during the course of this work.

Registry No. **1**, 500-72-1; **2**, 53882-05-6; **3**, 53882-12-5; *o*-cyanooxanilic acid, 61068-77-7; *o*-fluorooxanilic acid, 84944-15-0; *o*-chlorooxanilic acid, 77901-50-9.

Supplementary Material Available: Electron populations and bond orders for orbitals in the σ (Table II) and π (Table III) systems of molecules **1–3** (4 pages). Ordering information is given on any current masthead page.